3490 J. Agric. Food Chem. 2009, 57, 3490–3499
DOI:10.1021/jf900124r

JOURNAL OF AGRICULTURAL AND FOOD CHEMISTRY
ARTICLE

Myricetin Suppresses Invasion and Migration of Human Lung Adenocarcinoma A549 Cells: Possible Mediation by Blocking the ERK Signaling Pathway

YUAN-WEI SHIH,[†] PEI-FEN WU,[‡] YI -CHIEH LEE,[†] MING-DER SHI,[§] AND TAI-AN CHIANG*,[#]

[†]Department of Biological Science and Technology and Institute of Biomedical Science, Chung Hwa University of Medical Technology, No. 89 Wen-Hwa First Street, Jen-Te, Tainan 717, Taiwan, ROC, [‡]Department of Occupational Safety and Hygiene, Tajen University, No. 20 Wei-Sin Road, Yan-Pu, Pingtung 907, Taiwan, ROC, [§]Department of Medical Technology, Yongkang Veterans Hospital, No. 427 Fu-Xing Road, Yong-Kang, Tainan 710, Taiwan, ROC, and [#]Department of Medical Technology and Institute of Biological Science and Technology, Chung Hwa University of Medical Technology, No. 89 Wen-Hwa First Street, Jen-Te, Tainan 717, Taiwan, ROC

Cancer metastasis, involving multiple processes and various cytophysiological changes, is a primary cause of cancer death and may complicate clinical management, even leading to death. Myricetin (3,5,7,3′,4′,5′-hexahydroxyflavone), a naturally occurring flavonoid, has various anticancer activities. This is the first study to explore the antimetastatic effect of myricetin in human adenocarcinoma A549 cells in vitro. First, myricetin exerted a dose- and time-dependent inhibitory effect on the adhesion, invasion, and migration of A549 cells in the absence of cytotoxicity. Gelatin or casein zymography assays showed that myricetin inhibited the matrix metalloproteinase-2 (MMP-2) and urokinase-plasminogen activator (u-PA) activities of A549 cells. Moreover, myricetin also exerted an inhibitory effect on the phosphorylation of extracellular signal-regulated kinases 1 and 2 (ERK1/2) and inhibition of activation of nuclear factor kappa B (NF-κB), c-Fos, and c-Jun. Treatment with myricetin of A549 cells also led to a dose-dependent effect on the binding abilities of NF-κB and AP-1. Furthermore, the ERK inhibitor (U0126) could result in reduced activities of MMP-2 and u-PA concomitantly with a marked inhibition on cell invasion and migration. These results demonstrated that the inhibition of MMP-2 and u-PA expression by myricetin may be through a suppression on ERK1/2 phosphorylation and inhibit A549 cells invasion and migration. As shown by the above results, myricetin may be a powerful candidate in developing preventive agents for cancer metastasis.

KEYWORDS: Myricetin; migration; invasion; MMP-2; u-PA; ERK1/2; NF-κB; AP-1

INTRODUCTION

Flavonoids are a broadly distributed class of plant pigments, universally present in vascular plants and responsible for much of the coloring in nature (*1*). Myricetin (3,5,7,3′,4′,5′-hexahydroxyflavone, **Figure 1**), a flavonoid commonly found in tea, wines, berries, fruits, and medicinal plants, has been reported to possess antioxidative, antiproliferative, and anti-inflammatory effects (*2*−*4*). Previous studies showed that myricetin exerted an antiproliferative effect on lung, esophageal, leukemia, and prostate cancer cells (*5*−*8*). Other reports in JB6 P+ mouse epidermal cells have indicated that myricetin has a chemopreventive effect through inhibiting COX-2 expression by blocking the activation of NF-κB (*9*). Furthermore, a recent study showed that myricetin possesses inhibitory effects on MMP-2 pro tein expression and enzyme activity in colorectal carcinoma cells (*10*). Although it occurred by inducing cancer cells toward apoptosis, the precise impact and related molecular mechanism of myricetin on migration and invasion were still unclear.

Lung cancer is the major cause of malignancy-related deaths worldwide, and its incidence is rising in many countries (*11*). Approximately 40% of lung cancers are adenocarcinoma. Adenocarcinoma, which belongs to the subgroup of the non-small-cell lung cancers, is the most common type in the United States and Asia (*12*). Adenocarcinoma commonly develops resistance to radiation and chemotherapy, and often presents at stages too late for surgical intervention, resulting in a low overall survival at 5 years of $<15\%$ (*13*). Often, local invasion or migration to distant organs has already occurred by the time of the diagnosis. In many types of neoplasm, including lung cancer, higher levels of activated MMPs have been demonstrated in more invasive and/or metastatic tumors and many give prognostic information independent of stage (*14*).

*Corresponding author (telephone +886 6 2674567, ext. 450; fax +886 6 2605598; e-mail giantful@mail.hwai.edu.tw).

 Published on Web 3/30/2009

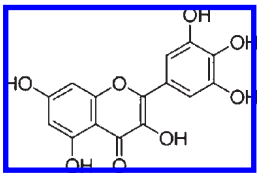

Figure 1. Chemical structure of myricetin.

Many papers have addressed the importance of interactions between cells and the extracellular matrix (ECM), which could enhance cell migration, invasion, proliferation, and ECM degradation. Metastasis has been found to be accompanied by various physiological alterations involved in the degradation of ECM, such as the overexpression of proteolytic enzyme activity, such as matrix metalloproteinases (MMPs) and u-PA, as well as the migration and invasion of tumor cells into the bloodstream or lymphatic system to spread to other tissues or organs (*15*, *16*). Two members of the zinc-dependent endopeptidases of the MMP family, the 72-kDa type IV collagenase (MMP-2) and the 92-kDa type IV collagenase (MMP-9), have been associated with tumor cell invasion and metastasis due to their ability to hydrolyze various ECMs (*17*, *18*). In addition, u-PA may initiate the activation of an enzymatic cascade and converts the zymogen plasminogen to plasmin (*19*). Meanwhile, the activation of these enzymes enables the degradation of the ECM by tumor cells, allowing their access to the vasculature, migration, and invasion into the target organ, and development of tumor metastasis (*20*). Moreover, MMPs or u-PA gene expression is chiefly regulated at the transcriptional [through AP-1 or NF-κB via mitogen activated protein kinase (MAPK) or PI3K/Akt pathway] and posttranscriptional levels and at the protein level by their activators or inhibitors and their cell surface localization (*21*, *22*). Therefore, MMPs, u-PA, and their regulatory pathways have been considered to be promising targets for anticancer drugs and chemopreventive agents.

Cancer metastasis is highly related to degradation of ECM, intercellular adhesion, and cellular motility. The objective of this work was to examine the inhibitory effects of myricetin on MMPs and u-PA activities. Also, the MAPK and Akt activities were examined on the highly metastatic A549 cells to explore the underlying mechanism for the involvement of myricetin in cancer invasion and migration in vitro.

MATERIALS AND METHODS

Materials. Myricetin (96% purity), DMSO, Tris-HCl, EDTA, SDS, phenylmethanesulfonyl fluoride, bovine serum albumin (BSA), gelatin, casein, plasminogen, type I collagen, crystal violet, leupeptin, Nonidet P-40, deoxycholic acid, sodium orthovanadate, and U0126 were purchased from Sigma-Aldrich (St. Louis, MO); protein assay kit was obtained from Bio-Rad Laboratories (Hercules, CA). Dulbecco's phosphate buffer solution (PBS), trypsin−EDTA, and powdered Dulbecco's modified Eagle's medium (DMEM) were purchased from Gibco/BRL (Gaithersburg, MD). Matrigel was from BD Biosciences (Bedford, MA). Antibodies against PKB/Akt, MAPK/ERK1/2, p38 MAPK, and JNK/SAPK, proteins, and phosphorylated proteins were purchased from Cell Signaling Technology (Beverly, MA). NF-κB (p65), c-Fos, c-Jun, β-actin, and C23 antibodies were from BD Transduction Laboratories (San Diego, CA). The enhanced chemiluminescence (ECL) kit was purchased from Amersham Life Science (Amersham, U.K.).

Cell Culture and Myricetin Treatment. A549, a human lung adenocarcinoma cell line, was obtained from BCRC (Food Industry Research and Development Institute, Hsin-Chu, Taiwan). Cells were cultured in DMEM supplemented with 10% fetal calf serum, 100 U/mL of penicillin, and 100 mg/mL streptomycin mixed antibiotics and 1 mM sodium pyruvate. All cell cultures were maintained at 37 °C in a humidified atmosphere of 5% CO_2−95% air. The culture medium was renewed every 2−3 days. Adherent cells were detached by incubation with trypsin. For myricetin treatment, the stock solution of myricetin was dissolved in dimethyl sulfoxide (DMSO) and sterilized by filtration through 0.2 μm disk filters. Appropriate amounts of stock solution (1 mg/mL in DMSO) of myricetin were added to the cultured medium to achieve the indicated concentrations (final DMSO concentration was $<0.2\%$) and then incubated with cells for the indicated time periods.

Analysis of Cell Viability (MTT Assay). To evaluate the cytotoxicity of myricetin, an MTT [3-(4,5-dimethylthiazol-2-yl)-2,5-diphenyltetrazolium bromide] assay was performed to determine cell viability. Briefly, cells were seeded at a density of 4×10^4 cells/mL in a 24-well plate for 24 h. Then, the cells were treated with myricetin at various concentrations (0, 5, 10, 20, 30, 40, and 50 μM) for various periods of time (24 and 48 h). Each concentration was repeated three times. After the exposure period, the medium was removed and followed by washing the cells with PBS. Then, the medium was changed and incubated with MTT solution (5 mg/mL)/well for 4 h. The medium was removed, and formazan was solubilized in isopropanol and measured spectrophotometrically at 563 nm. The percentage of viable cells was estimated by comparison with the untreated control cells.

Cell−Matrix Adhesion Assay. Cells were seeded on a 24-well plate and coated with 150 μL of type I collagen (10 μg/mL); then they were cultured for 30 min. Afterward, nonadherent cells were removed by PBS washes, and adherent cells were fixed in ethanol. After a staining with 0.1% crystal violet, fixed cells were lysed in 0.2% Triton-100 and measured spectrophotometrically at 550 nm.

Wound-Healing Assay. For cell motility determination, A549 cells (1×10^5cells/mL) were seeded in a 6-well tissue culture plate and grown to 80−90% confluence. After aspiration of the medium, the center of the cell monolayers was scraped with a sterile micropipet tip to create a denuded zone (gap) of constant width. Subsequently, cellular debris was washed with PBS, and A549 cells were exposed to various concentrations of myricetin (0, 5, 10, and 20 μM). Wound closure was monitored and photographed at 0, 12, 24, 36, and 48 h with an Olympus CKX-41 inverted microscope and an Olympus E-410 camera. To quantify the migrated cells, pictures of the initial wounded monolayers were compared with the corresponding pictures of cells at the end of the incubation. Artificial lines fitting the cutting edges were drawn on pictures of the original wounds and overlaid on the pictures of cultures after incubation. Cells that had migrated across the white lines were counted in six random fields from each triplicate treatment, and data are presented as mean ± SD.

Boyden Chamber Invasion and Migration Assay. The ability of A549 cells to pass through matrigel-coated filters was measured by the Boyden chamber invasion assay. Matrigel (BD Biosciences, Bedford, MA) was diluted to 200 μg/mL with cold-filtered distilled water and applied to the top side of the 8 μm pore polycarbonate filter. Briefly, A549 cells were treated with various concentrations of myricetin for 48 h or with 5 μM myricetin for 6, 12, 24, and 48 h. Then, cells were detached by trypsin and resuspended in serum-free medium. Medium containing 10% FBS was applied to the lower chamber as a chemoattractant, and then cells were seeded on the upper chamber at a density of 1×10^5 cells/well in 50 μL of serum-free medium. The chamber was incubated for 8 h at 37 °C. At the end of incubation, cells in the upper surface of the membrane were carefully removed with a cotton swab, and cells that had invaded across the matrigel to the lower surface of the membrane were fixed with methanol and stained with 5% Giemsa solution. The invasive cells on the lower surface of the membrane filter were counted with a light microscope. The data are presented as the average number of cells attached to the bottom surface from randomly chosen fields. Each experiment was carried out in triplicate.

To measure the ability of A549 cells on migration, cells were seeded into the Boyden chamber with 8 μm pore polycarbonate filters, which were not coated with matrigel. Migrative cells

were treated with various concentrations of myricetin for 48 h or with 5 μM myricetin for 6, 12, 24, and 48 h. The migration assay was measured as described for the invasion assay.

Analysis of MMP-2, MMP-9, and u-PA Activities by Zymography. The activities of MMP-2 and MMP-9 were assayed by gelatin zymography. Briefly, conditioned media from cells cultured in the absence of serum for 24 h were collected. Samples were mixed with loading buffer and electrophoresed on 8% SDS−polyacrylamide gel containing 0.1% gelatin. Electrophoresis was performed at 140 and 110 V for 3 h. Gels were then washed twice in Zymography washing buffer (2.5% Triton X-100 in double-distilled H_2O) at room temperature to remove SDS, followed by incubation at 37 °C for 12−16 h in Zymography reaction buffer [40 mM Tris-HCl (pH 8.0), 10 mM $CaCl_2$, 0.02% NaN_3], staining with Coomassie blue R-250 (0.125% Coomassie blue R-250, 0.1% amino black, 50% methanol, 10% acetic acid) for 1 h, and destaining with destaining solution (20% methanol, 10% acetic acid, 70% double-distilled H_2O). Nonstaining bands representing the levels of the latent forms of MMP-2 and MMP-9 were quantified by densitometer measurement using a digital imaging analysis system.

Visualization of u-PA activity was performed by casein−plasminogen zymography. Briefly, 2% casein and 20 μg/mL plasminogen were added to 8% SDS-PAGE gel. Samples with a total protein of about 20 μg were then loaded onto the gels. The u-PA activity of cells treated or untreated with myricetin was measured as described for gelatin zymography.

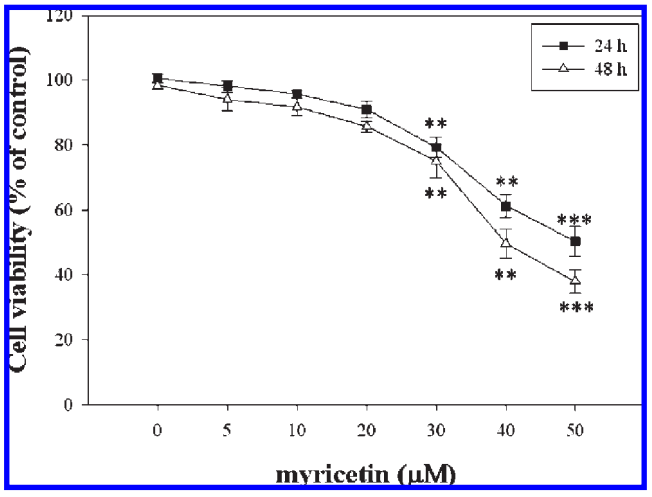

Figure 2. Effect of myricetin on the viability of A549 cells. A549 cells (4×10^4 cells/mL) were treated with various concentrations (0, 5, 10, 20, 30, 40, and 50 μM) of myricetin for 24 and 48 h. Cell viability was determined by MTT assay. The survival cell number was directly proportional to formazan, which was measured spectrophotometrically at 563 nm. Values are expressed as mean ± SD of three independent experiments. **, $p < 0.01$, and ***, $p < 0.001$, compared with the untreated control (dose 0).

Preparation of Whole-Cell Lysates and Nuclear Extracts. The cells were lysed with iced-cold RIPA buffer (1% NP-40, 50 mM Tris-base, 0.1% SDS, 0.5% deoxycholic acid, 150 mM NaCl, pH 7.5), and then phenylmethanesulfonyl fluoride (10 mg/mL), leupeptin (17 mg/mL), and sodium orthovanadate (10 mg/mL) were added. After vortexing for 30 min on ice, the samples were centrifuged at 12000*g* for 10 min. Then the supernatants were collected, denatured, and subjected to SDS-PAGE and Western blotting. Nuclear extracts were prepared as previously described and then used for NF-κB, c-Fos, c-Jun, and AP-1 detection. Each nuclear pellet was resuspended in nuclear extract buffer (1.5 mM $MgCl_2$, 10 mM HEPES, pH 7.9, 0.1 mM EDTA, 0.5 mM dithiothreitol, 0.5 mM phenylmethanesulfonyl fluoride, 25% glycerol, and 420 mM NaCl). The nuclear suspension was incubated on ice for 20 min and then centrifuged at 14000*g* for 5 min. The supernatant (corresponding to the soluble nuclear fraction) was saved, and the remaining pellet was solubilized by sonication in PBS. The protein content was determined with Bio-Rad protein assay reagent using bovine serum albumin as standard.

Western Blotting Analysis. To analyze the metastasis-related proteins, Western blotting was performed as follows. The denatured samples (50 μg of purified protein) were resolved on 10−12% SDS-PAGE gels. The proteins were then transferred onto nitrocellulose membranes. Nonspecific binding of the membranes was blocked with Tris-buffered saline (TBS) containing 1% (w/v) nonfat dry milk and 0.1% (v/v) Tween-20 (TBST) for more than 2 h. Membranes were washed with TBST three times for 10 min and incubated with an appropriate dilution of specific primary antibodies in TBST overnight at 4 °C. Subsequently, the membranes were washed with TBST and incubated with appropriate secondary antibody (horseradish peroxidase-conjugated goat anti-mouse or anti-rabbit IgG) for 1 h. After the membrane had been washed three times for 10 min in TBST, band detection was revealed by enhanced chemiluminescence using ECL Western blotting detection reagents and exposed ECL hyperfilm in a UVP Luminescent image analyzer.

Analysis of NF-κB and AP-1 Binding Assay (Electrophoretic Mobility Shift Assay). Cell nuclear proteins were extracted with a nuclear extract buffer and measured by an electrophoretic mobility shift assay (EMSA). Cells (1×10^5/mL) were collected in PBS buffer (pH 7.4) and centrifuged at 2000*g* for 5 min at 4 °C. Cells were lysed with buffer A [10 mM HEPES, 1.5 mM $MgCl_2$, 10 mM KCl, 0.5 mM DTT, and 0.5 mM PMSF (pH 7.9) containing 5% NP-40] for 10 min on ice, and this was followed by vortexing to shear the cytoplasmic membranes. The lysates were centrifuged at 2000*g* for 10 min at 4 °C. The pellet containing the nuclei was extracted with high-salt

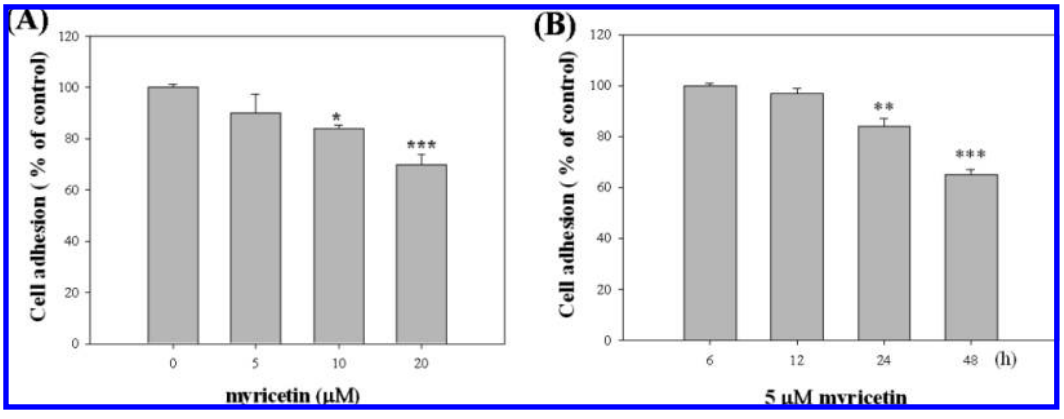

Figure 3. Concentration- and time-dependent effects of myricetin on cell−matrix adhesion of A549 cells. In a concentration-dependent assay (**A**), A549 cells were treated with various concentrations (0, 5, 10, and 20 μM) of myricetin for 24 h. In a time-dependent assay (**B**), A549 cells were treated with 5 μM myricetin for 6, 12, 24, and 48 h. Treated cells were then subjected to analyses for cell−matrix adhesion as described under Materials and Methods. Values are expressed as mean ± SD of three independent experiments. *, $p < 0.05$, **, $p < 0.01$, and ***, $p < 0.001$, compared with the untreated control (dose 0).

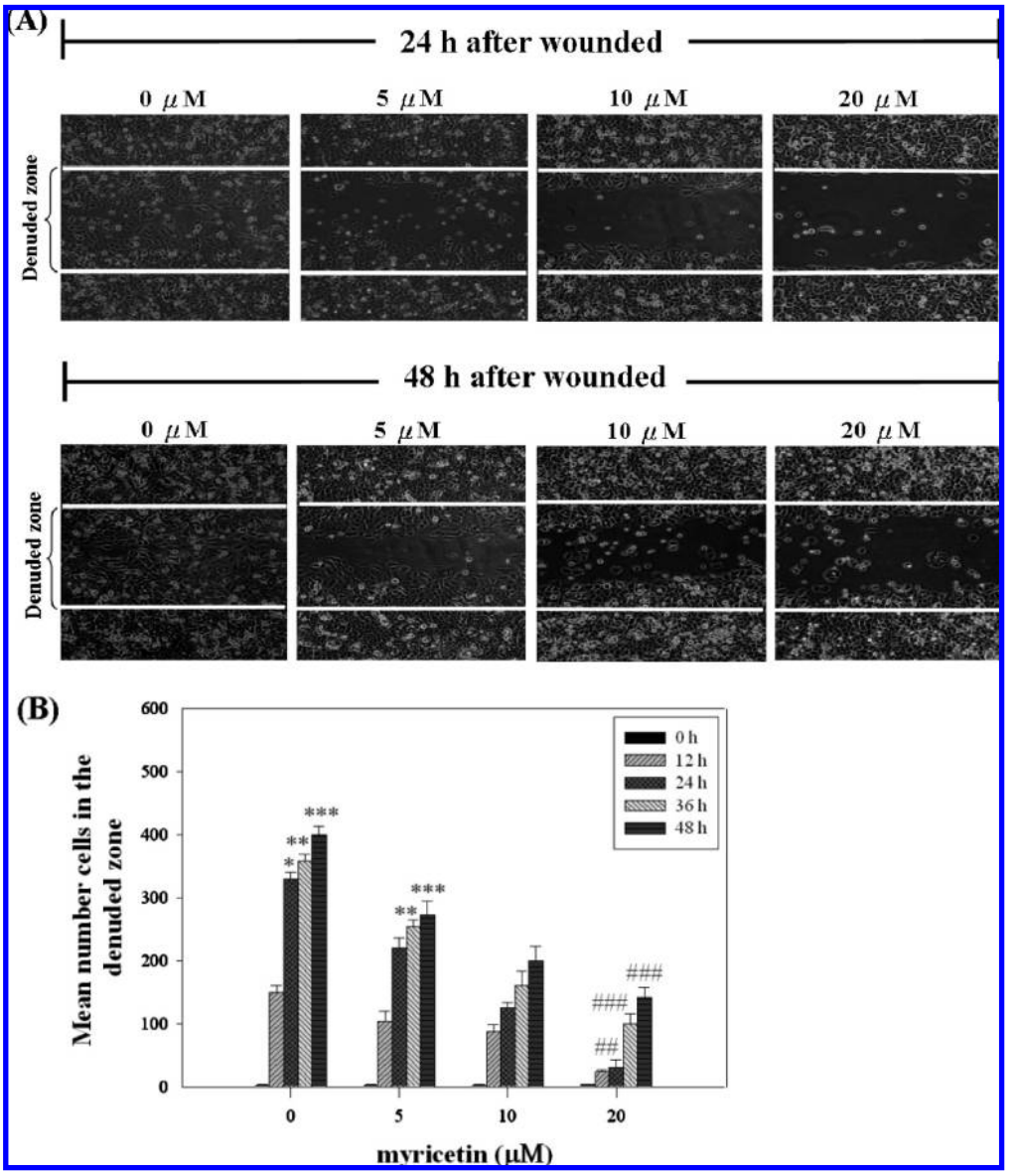

Figure 4. Effect of myricetin on the motility of A549 cells. (**A**) A549 cell monolayers were scraped by a sterile micropipette tip, and the cells were treated with various concentrations (0, 5, 10, and 20 μM) of myricetin for 0, 12, 24, 36, and 48 h. The number of cells in the denuded zone was quantitated after indicated times (0, 12, 24, 36, and 48 h) by inverted microscopy. White lines indicate the wound edge. Pictures only were presented 24 and 48 h. (**B**) Migrated cells across the white lines were counted in six random fields from each treatment. Quantitative assessment of the mean number of cells in the denuded zone is expressed as mean ± SD of three independent experiments. *, $p < 0.05$, **, $p < 0.01$, and ***, $p < 0.001$, compared with the untreated control (dose 0). ##, $p < 0.01$, and ###, $p < 0.001$, compared with 0 h-treated time.

buffer B (20 mM HEPES, 420 mM NaCl, 1.5 mM $MgCl_2$, 0.5 mM DTT, 0.5 mM PMSF, 0.2 mM EDTA, and 25% glycerol) for 15 min on ice. The lysates were clarified by centrifugation at 13000*g* for 10 min at 4 °C. The supernatant containing the nuclear proteins was collected and frozen at −80 °C until use. The protein content of nuclear fractions was determined with Bio-Rad protein assay. Five microgram aliquots of nuclear proteins were mixed with either biotin-labeled NF-κB or AP-1 oligonucleotide probes for 15 min at room temperature, oligonucleotides containing sense of NF-κB, 5′-AGTTGAGGGGACTTTCCCAGGC-3′, antisense of NF-κB, 3′-TCAACTCCCCTGA AAGGGTCCG-5′; sense of AP-1, 5′-CGCTTGATGACTCAGCCGGAA-3′, and antisense of AP-1, 3′-GCGAACTACTGAGTCGGCCTT. DNA probes were added to 10 μL binding reactions containing double-distilled H_2O, 5 μg of nuclear protein, 1 μL of poly (dI-dC), 1 μL of biotin-labeled double-stranded NF-κB or AP-1 oligonucleotides, and 2 μL of 10-fold binding buffer in a microcentrifuge tube and were incubated for 15 min at room temperature. Specific competition binding assays were performed by adding a 200-fold excess of unlabeled probe as a specific competitor. Following protein−DNA complex formation, samples were loaded on a 6% nondenaturing polyacrylamide gel in 0.5× TBE buffer and then transferred to positively charged nitrocellulose membranes (Milipore, Bedford, MA) by a transfer blotting apparatus and cross-linked in a Stratagene cross-linker. Gel shifts were visualized with streptavidin−horseradish peroxidase followed by chemiluminescent detection.

Statistical Analysis. Data are expressed as mean ± standard deviation of three independent experiments and analyzed by Student's *t* test (Sigmaplot 2001). Significant differences were established at $p \leq 0.05$.

RESULTS

Effect of Myricetin in A549 Cell Viability. In this study, we first examined the cytotoxicity of myricetin by treating A549 cells with myricetin at various concentrations (0, 5, 10, 20, 30, 40, and 50 μM) for 24 and 48 h followed by the MTT assay.

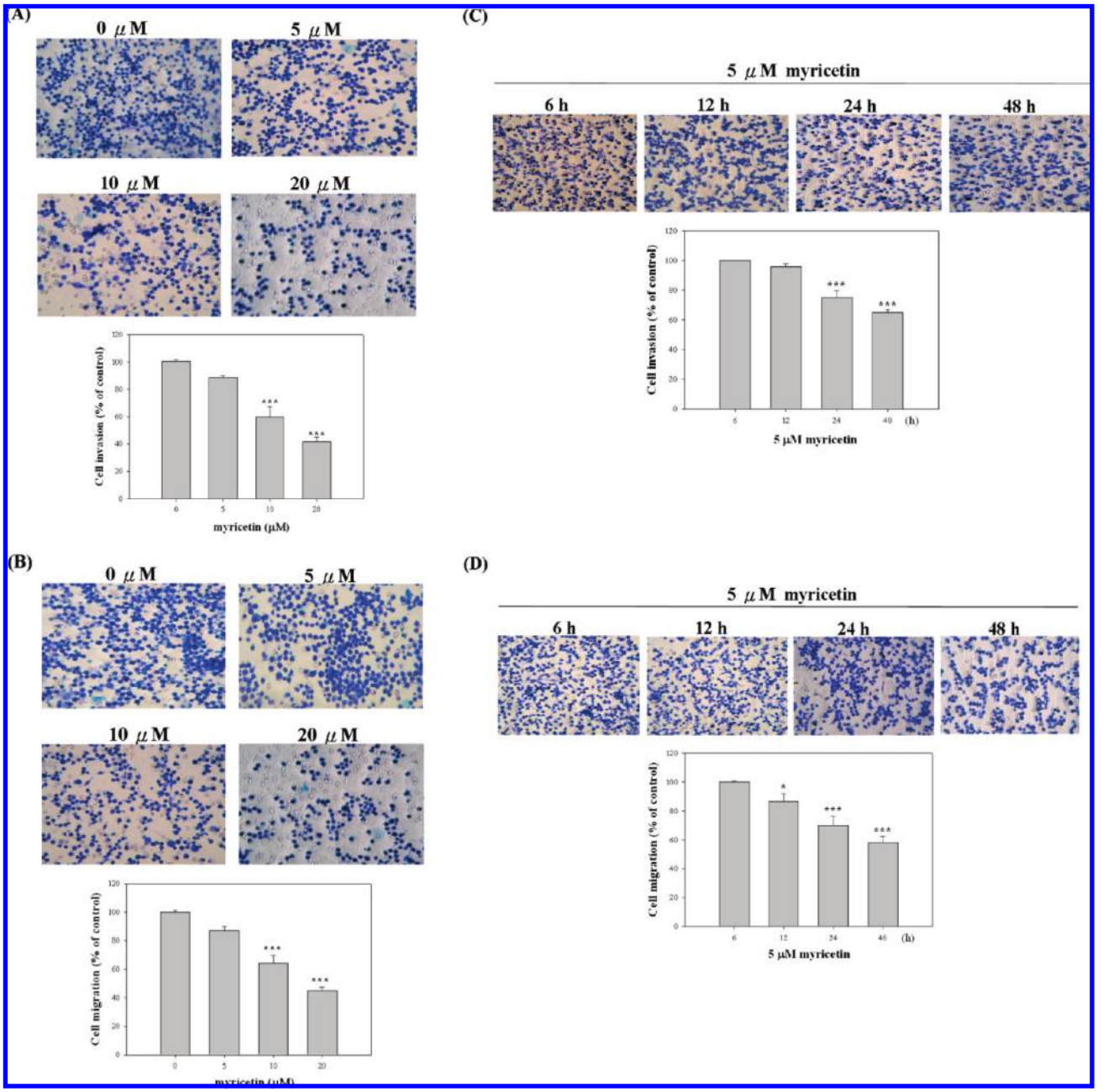

Figure 5. Concentration- and time-dependent effects of myricetin on invasion and migration of A549 cells. In concentration-dependent assays (**A**, **B**), A549 cells were treated with various concentrations (0, 5, 10, and 20 μM) of myricetin for 48 h. In time-dependent assays (**C**, **D**), cells were treated with 5 μM myricetin for 6, 12, 24, and 48 h. Cell invasion was measured by Boyden chamber for 8 h; polycarbonate filters (pore size = 8 μm) were precoated with matrigel. Cell migration was measured by Boyden chamber for 6 h with polycarbonate filters (pore size = 8 μm); invasion and migration abilities of A549 cells were quantified by counting the number of cells that invaded to the underside of the porous polycarbonate membrane under microscopy and represent the average of three experiments ± SD. $*$, $p < 0.05$, and $***$, $p < 0.001$, compared with the untreated control (dose 0).

As shown in **Figure 2**, the level of cell viability effect of myricetin was assayed in a dose- and time-dependent manner by the MTT assay. Compared to the untreated control, after 24 and 48 h, treatment with myricetin at a concentration between 0 and 20 μM was not significantly changed, indicating that myricetin was not toxic to A549 cells at these dosages. When cells were treated with 30−50 μM myricetin for 24 and 48 h, cell viability was significantly decreased. These results demonstrated that the treatment of myricetin at doses higher than 20 μM for 24 and 48 h resulted in dose- and time-dependent loss of cell viability in A549 cells, but doses lower than 20 μM for 24 and 48 h did not cause cytotoxicity. These doses below 20 μM of myricetin were applied in all subsequent experiments.

Myricetin Inhibited Adhesion, Migration, and Invasion in A549 Cells. To investigate the inhibitory effect of myricetin on A549 cells adhesion, migration, and invasion processes, a cell−matrix adhesion assay, a wound-healing assay, and a Boyden chamber assay were used. In the cell−matrix adhesion assay, myricetin showed a dose- and time-dependent inhibitory effect on the cell adhesion ability of A549 cells (**Figure 3A** and **3B**). For the wound-healing assay, according to a quantitative assessment, the cells were treated with various concentrations of myricetin for 0, 12, 24, 36, and 48 h. The results showed that 20 μM myricetin exhibited the greatest inhibition of cell motility after 48 h of incubation (**Figure 4A** and **4B**). Also, compared with the untreated cells, the level of A549 cell numbers decreased almost 3-fold after

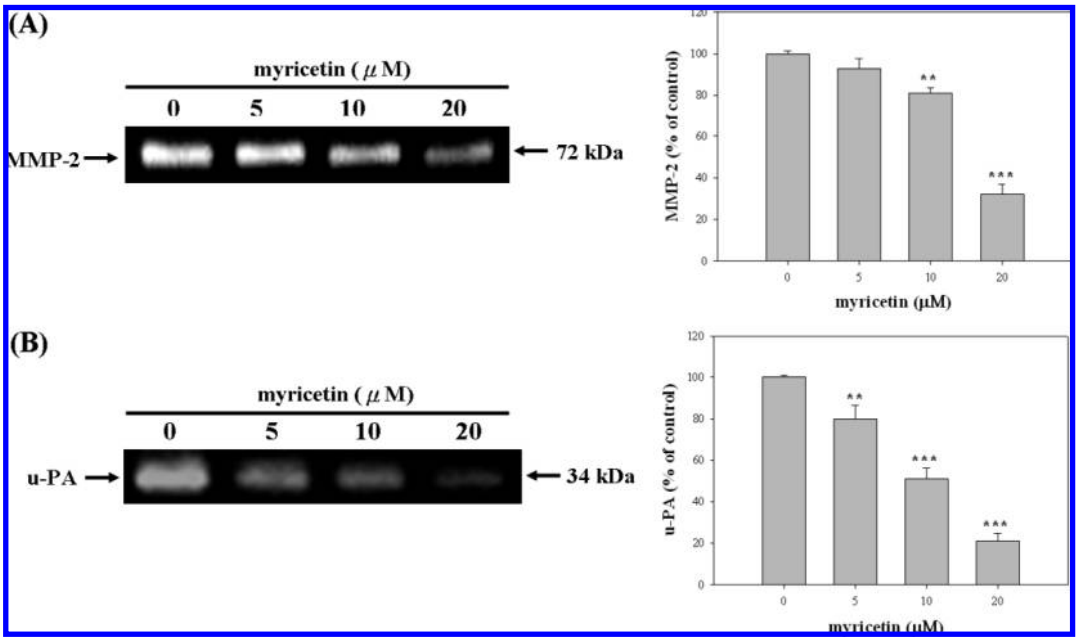

Figure 6. Effect of myricetin on MMP-2 and u-PA activities of A549 cells. Cells were treated with various concentrations (0, 5, 10, and 20 μM) of myricetin for 24 h. The conditioned media were collected, and MMP-2 and u-PA activities were determined by gelatin or casein zymography. MMP-2 and u-PA activities were quantified by densitomeric analysis. The densitomeric data were expressed as mean ± SD of three independent experiments. **, $p < 0.01$, and ***, $p < 0.001$, compared with the untreated control (dose 0).

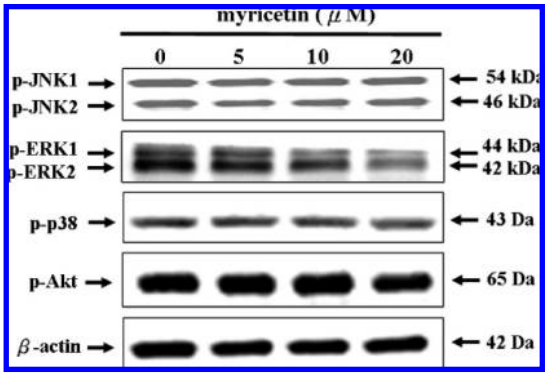

Figure 7. Inhibitory effect of myricetin on the phosphorylation of ERK1/2. Cells were treated with various concentrations (0, 5, 10, and 20 μM) of myricetin for 6 h, and then cell lysates were subjected to SDS-PAGE followed by Western blotting and immunoprobing with antiphospho-JNK1/2, antiphospho-ERK1/2, antiphospho-p38, and antiphospho-Akt antibodies. β-Actin was used as a loading control. The relative densities of phosphorylated forms of JNK, ERK, p38, and Akt were normalized to total values of JNK, ERK, p38, and Akt, which were determined by densitometric analysis. Results from three repeated and separated experiments were similar.

treatment with 20 μM myricetin for 48 h. These results revealed that myricetin significantly inhibited the motility of A549 cells.

One important characteristic of metastasis is the invasive and migratory ability of tumor cells. Using a cell invasion and migration assay with Boyden chamber, the reductions in invasion and migration of A549 cells were observed when the myricetin concentrations were beyond 5 μM. The results showed that myricetin induced a dose- and time-dependent decrease in invasion and migration with increasing concentration of myricetin. In the 20 μM myricetin-treated group, the invasion and migration of A549 cells showed 42 and 44% inhibition, respectively, compared with the non-myricetin-treated group (**Figure 5A** and **5B**). Subsequently, time course experiments with myricetin at a low concentration of 5 μM also indicated that myricetin could significantly inhibit the invasion and migration of A549 cells in a time-dependent manner (**Figure 5C** and **5D**). The results demonstrated that myricetin significantly inhibited the invasion and migration of highly metastatic A549 cells.

Myricetin Reduced MMP-2 and u-PA Activities in A549 Cells. To clarify if MMPs and u-PA are involved in the inhibition of invasion, migration, and adhesion by myricetin, the effects of myricetin on MMPs and u-PA activities were investigated by gelatin and casein zymography under a condition of serum starvation, respectively. As shown in **Figure 6A**, myricetin tremendously reduced MMP-2 activity in a dose-dependent manner, whereas u-PA activity was also inhibited by myricetin (**Figure 6B**). However, the impact of myricetin on MMP-9 activity was inconclusive because an extremely low level of MMP-9 was expressed in A549 cells, even in the absence of myricetin (data no shown). These results suggested that the antimetastatic effect of myricetin was related to the inhibition of enzymatically degradative processes of tumor metastasis. This study was the first to demonstrate the biochemical mechanism(s) by which myricetin reduced the metastasis in human lung adenocarcinoma cells. The activities of MMP-2 and u-PA have been shown to play a critical role in degrading the basement membrane in cancer invasion and migration.

Myricetin Inhibited ERK Phosphorylation in A549 Cells. Because we have shown that treating A549 cells with myricetin inhibited the cell metastasis and activities of MMP-2 and u-PA, the underlying mechanisms were further examined. Signals from extracellular stimuli are transmitted to the nucleus, involving the activation of kinases and mediation of signals from cell membrane receptor triggered by growth factors, cytokines, and cell−matrix interactions. Several studies have indicated the transcription factors (for example, NF-kB, c-Fos, c-Jun), JNK1/2, ERK1/2, p38 MAPK, and Akt are involved in the activities of MMP-2 and u-PA on different cell types (*23*−*25*). To assess whether myricetin

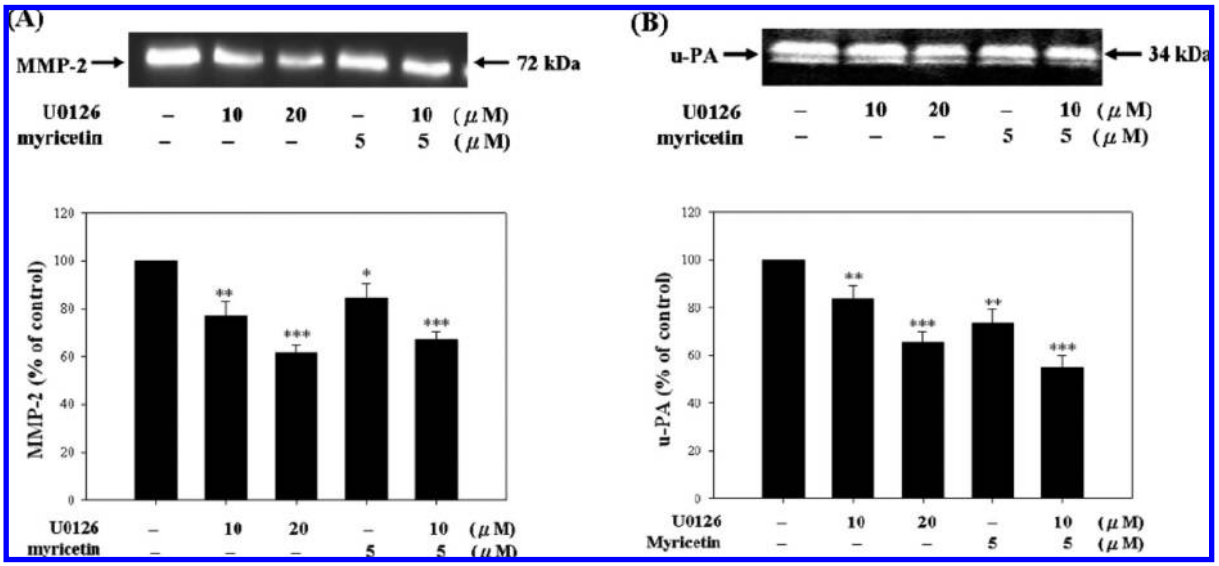

Figure 8. Effect of ERK inhibitor (U0126) and myricetin on the activities of MMP-2 and u-PA. Cells were plated in a 6-well and pretreated with U0126 (10 or 20 μM) for 1 h and then incubated in the presence or absence of myricetin (5 μM) for 24 h. Afterward, the culture medium was subjected to gelatin and casein zymography to analyze the activities of (**A**) MMP-2 and (**B**) u-PA. The determined activities of these proteins were subsequently quantified by densitometric analysis with that of control being 100% as shown just below the gel data. Data represent the mean ± SD of three independent experiments (∗, $p < 0.05$, ∗∗, $p < 0.01$, and ∗∗∗, $p < 0.001$).

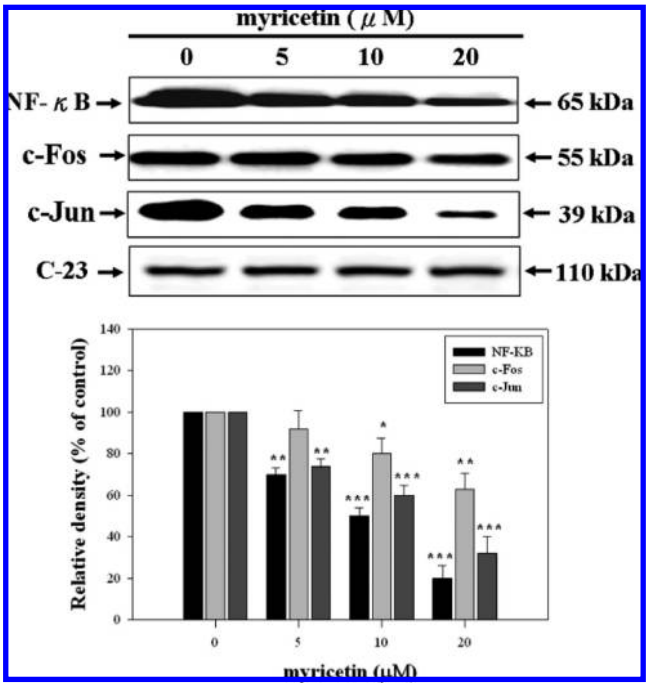

Figure 9. Effect of myricetin on the nuclear levels of NF-κB, c-Fos, and c-Jun. A549 cells were treated with various concentrations (0, 5, 10, and 20 μM) of myricetin for 24 h. Cell nuclear extracts were prepared and analyzed by Western blotting with anti-NF-κB (p65), c-Fos, and c-Jun antibodies. C23 was a nucleus protein loading control. It was determined that the nuclear levels of NF-κB, c-Fos, and c-Jun were subsequently quantified by densitometric analysis with that of control being 1-fold. The densitometric results are expressed as mean ± SD of three independent experiments. ∗, $p < 0.05$, ∗∗, $p < 0.01$, and ∗∗∗, $p < 0.001$, compared with the untreated control.

mediates and/or inhibits phosphorylation of JNK1/2, ERK1/2, p38, and Akt, we examined the effect of myricetin on the phosphorylated status of MAPK family members (JNK1/2, ERK1/2, p38) and Akt in A549 cells that had been treated with various concentrations of myricetin for 6 h. **Figure 7** shows that myricetin significantly inhibited the activation of ERK1 and ERK2 as shown by decreasing the phosphorylation of ERK1 and ERK2, whereas it had no significant effect on JNK1/2, p38, and Akt activities. Moreover, no significant change in the total amount of ERK1/2, JNK1/2, p38, and Akt proteins was observed (data not shown).

To further investigate whether the inhibition of myricetin was mainly through inhibition of the ERK1/2 signaling pathway, A549 cells were pretreated with a ERK inhibitor (U0126; 10 or 20 μM) for 1 h and then incubated in the presence or absence of myricetin (5 μM) for 24 h. Results of the gelatin zymography assay showed that a sole treatment of U0126 (10 or 20 μM) or myricetin (5 μM), respectively, reduced the activity of MMP-2 by 23, 39, and 15%, and the combination treatment (10 μM U0126 + 5 μM myricetin) could reduce MMP-2 secretion by 33% (**Figure 8A**). Similarly, in a casein zymography assay, a sole treatment of U0126 (10 or 20 μM) or myricetin (5 μM) reduced the activity of u-PA by 16, 34, and 26%, respectively, and the combination treatment (10 μM U0126 + 5 μM myricetin) could further reduce the secretion of u-PA by 45% (**Figure 8B**). Indeed, as shown in **Figure 7** and **Figure 8**, myricetin could inhibit the phosphorylation of ERK1/2, and the involvement of the MAPK pathway was further supported by using the ERK inhibitor in our experimental model. Treatment with an inhibitor of ERK could inhibit MMP-2 and u-PA secretion as well as reduction cell invasion and migration.

Myricetin Inhibited the Nuclear Levels of NF-κB, c-Fos, and c-Jun. NF-κB and AP-1 families of transcriptional factors have been known to translocate to the nucleus and regulate numerous genes involved in MMPs or u-PA secretion. To further explore the nuclear protein levels of NF-κB, c-Fos, and c-Jun, A549 cells were treated with myricetin of various concentrations (0, 5, 10, and 20 μM) for 24 h by Western blotting, and the possible inhibitions of myricetin on NF-κB, c-Fos, and c-Jun were analyzed. As explained in **Figure 9**, the nuclear levels of NF-κB, c-Fos, and c-Jun were gradually diminished by treatment with

myricetin compared to 0 μM after 24 h. The data have shown especially inhibition by a treatment with 20 μM myricetin.

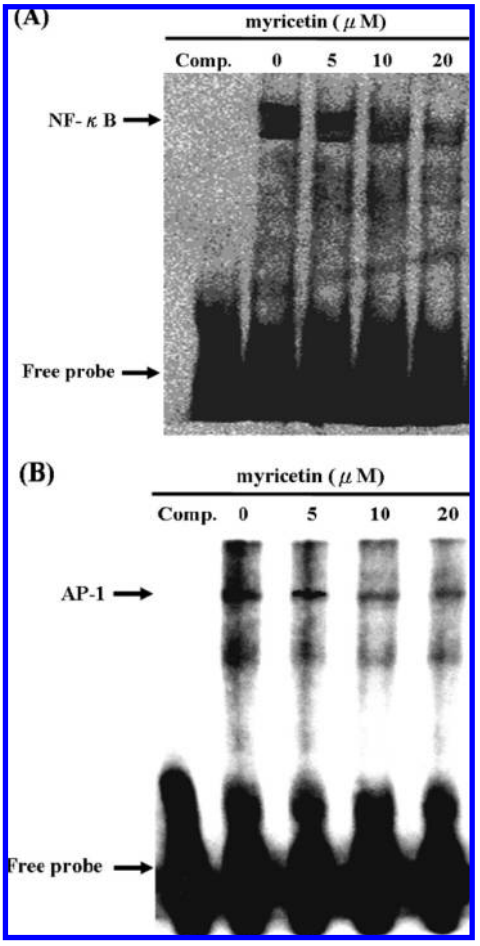

Figure 10. Effect of myricetin on the DNA binding activities of NF-κB and AP-1. A549 cells were treated with various concentrations (0, 5, 10, and 20 μM) of myricetin for 24 h, and then nuclear extracts were prepared and analyzed for (**A**) NF-κB and (**B**) AP-1 DNA binding activity using biotin-labeled consensus NF-κB and AP-1 specific oligonucleotides, and then EMSA assay was performed as described under Materials and Methods. Lane 1: nuclear extracts incubated with 100-fold excess of unlabeled consensus oligonucleotide (comp.) to confirm the specificity of binding. Excess free probe is indicated at the bottom. Results from three repeated and separate experiments were similar.

Myricetin Inhibited the DNA Binding Activities of NF-κB and AP-1. Previous papers have demonstrated that the MMP-2 and u-PA promoters have several transcription-binding motifs, including NF-κB and AP-1 (*26*). Thus, multiple pathways leading to activation of NF-κB and AP-1 binding factors in tumor cells may contribute to MMP-2 and u-PA transcription and metastatic enhancement. In another study, to clarify the involvement of NF-κB and AP-1 proteins in the mechanism of myricetin's action, the effect of myricetin on the DNA binding activities of NF-κB and AP-1 in A549 cells was investigated by EMSA. As shown in **Figure 10A** and **Figure 10B**, A549 cells treated with 0−20 μM myricetin for 24 h showed that myricetin inhibited NF-κB and AP-1 transcriptional activity in a dose-dependent manner. The binding activities of NF-κB and AP-1 were especially inhibited by a treatment with 20 μM myricetin.

Myricetin Inhibited Cell Invasion and Migration through an Inactivation of the ERK1/2 Signaling Pathway. To further delineate whether the inhibition of cell invasion and migration by myricetin occurred mainly through an inhibition of ERK1/2 signaling, A549 cells were pretreated with a ERK inhibitor (U0126; 20 μM) and then incubated in the presence or absence of myricetin (5 μM) for 48 h. Compared with the control, the invasion and migration assays revealed sole treatment with myricetin or U0126 decreased cell invasion and migration by 42 and 34% and by 54 and 38%, respectively, and the combination treatment (20 μM U0126 + 5 μM myricetin) could further reduce cell invasion and migration by 55 and 68%, respectively (**Figure 11A** and **Figure 11B**).

DISCUSSION

In this study, we explored the antimetastatic mechanism of myricetin on the invasion/migration of human adenocarcinoma A549 cells and found that myricetin can inhibit the invasion and migration of A549 cells in vitro model. We have demonstrated myricetin inhibition of A549 cells may occur through inactivation of the ERK signaling pathway, exerting inhibitory effects on NF-κB, c-Fos, and c-Jun transcriptional factors and inhibiting NF-kB and AP-1 DNA binding activity, thereby decreasing the activities of MMP-2 and u-PA and then having an antimetastatic effect in the cells. Our results strengthen the potential of myricetin as a new strategy for anticancer therapy.

Metastasis is the major cause of death among cancer patients. It requires several sequential steps, including various

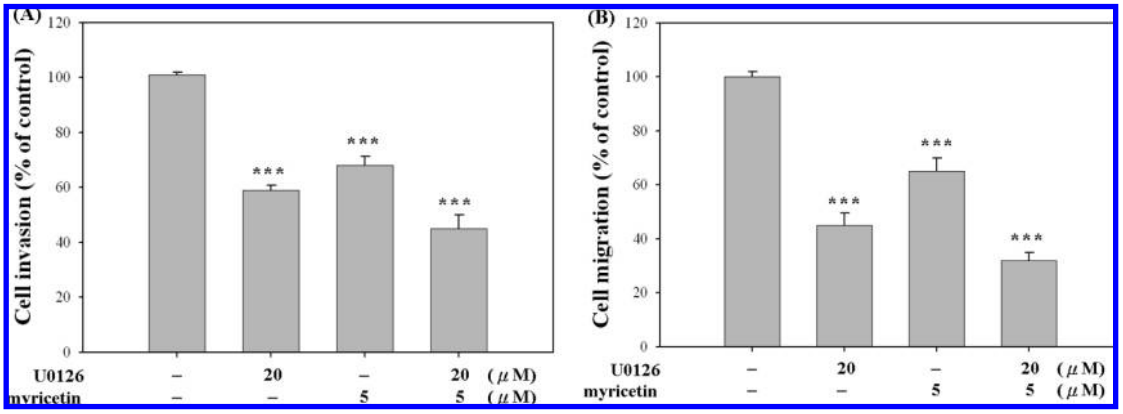

Figure 11. Effect of ERK inhibitor (U0126) and myricetin on cell invasion and migration. Cells were plated in a 6-well and pretreated with U0126 (20 μM) for 1 h and then incubated in the presence or absence of myricetin (5 μM) for 48 h. Afterward, cells were subjected to analyses for invasion and migration as described under Materials and Methods. Data represent the mean ± SD of three independent experiments (***, $p < 0.001$).

physiological alterations involved in cell−ECM interaction, separation of single cells from solid tumor tissue, and degradation of ECM by overexpression of proteolytic enzyme activity, such as the matrix metalloproteinases. Meanwhile, locomotion of tumor cells into the extracellular matrix and invasion of lymph and blood vessels occur, and the migrated tumor cells concomitantly escape the immunologic system in the circulation, exit to the new tissue, and eventually colonize a distant site (*27*). In recent years, attention has been drawn to the physiological relevance of MMPs and u-PA, markers related to the metastatic ability and malignancy of tumor cells. Thus, many studies have shown that proteinases related to the degradation of matrix are required for tumor cell metastasis, and enhanced production of MMPs and u-PA correlates with invasion, migration, and angiogenesis of the tumors. To further explore the exact expression of myricetin-induced inhibition on the invasion and migration, we performed gelatin or casein−plasminogen zymographic assays to detect activities of MMP-2, MMP-9, and u-PA. The result showed myricetin notably down-regulated activities of MMP-2 and u-PA. These results demonstate that the antimetastastic effect of myricetin was associated with the inhibition of enzymatically degradative processes of tumor metastasis. Such effects of MMPs and u-PA are not exclusive to myricetin, because similar results have been observed for genistein, ursolic acid, and berberine (*26*, *28*, *29*). Furthermore, we used a wound-healing assay and a Boyden chamber assay to quantify the migratory potential of A549 cells. These suggested that myricetin significantly inhibited the invasion and migration of A549 cells.

A major mechanism through which signals from extracellular stimuli are transmitted to the nucleus involves activation of kinases. These kinases, serine/threonine kinases related to the mitogen-activated proteins kinase (MAPK) superfamily, mediate signals from cell membrane receptors triggered by growth factors, cytokines, and cell−matrix interactions. MAPKs are intricately involved in the expression of the components involved in MMPs or u-PA promoter induction via NF-kB, AP-1, and its association with c-Fos and c-Jun. At least three subgroups of MAPK family members have been implicated: extracellular signal-regulated kinases (ERKs), c-Jun N-terminal kinase/stress-activated protein kinase (JNK/SAPK), and p38 MAPK. Indeed, we have demonstrated that treatment with myricetin inhibited phosphorylation of ERK. In contrast, myricetin did not significantly affect phospho-p38 and JNK1/2 activity. The involvement of the MAPK pathway was further supported by utilizing the ERK inhibitor in our experimental model. A treatment with a specific inhibitor for ERK could inhibit MMP-2 and u-PA secretion. Because several studies on different cell types suggested the ERK1/2 seems to play a central role in regulating the activities of MMPs or u-PA (*21*−*23*), inhibition of the ERK1/2 pathway might have the potential to prevent angiogenesis, proliferation, invasion, and migration for a wide range of tumors.

The transcription of MMPs and u-PA genes is regulated by upstream regulatory sequences, including NF-κB, AP-1, and Ets-1 binding sites (*26*, *30*). Therefore, our work provides insight on how myricetin suppressed the ERK signaling pathway and reduced NF-kB and AP-1 transcriptional activities in A549 lung adenocarcinoma cells. Indeed, one or more of these binding sites have been implicated in mediating the effects of a diverse set of agents. Here, we have also found that the treatment with myricetin of A549 cells results in an inhibition of NF-kB and AP-1 DNA binding activities, which was accompanied by the inhibition of nuclear translocation of these factors.

In conclusion, we have demonstrated here the inhibitory effects of myricetin on the invasion and migration of A549 cells, which may be through an inactivation of the ERK signaling pathway. In the future, the effects of myricetin on the metastasis of A549 cells in vivo will be examined further. This study suggests myricetin may serve as an efficient antimetastatic drug in cancer treatment.

ABBREVIATIONS USED

MMPs, matrix metalloproteinases; u-PA, urokinase-type plasminogen activator; ECM, extracellular matrix; MAPK, mitogen-activated protein kinase; ERK, extracellular signaling-regulating kinase; JNK/SAPK, c-Jun N-terminal kinase/stress-activated protein kinase; PI3K, phosphoinositide 3-kinase; NF-κB, nuclear factor kappa B; AP-1, activator protein-1; IκB, inhibitor of NF-κB.

LITERATURE CITED

(1) Cody, V. Crystal and molecular structures of flavonoids. *Prog. Clin. Biol. Res.* **1998**, *280*, 29–44.
(2) Aherne, S. A.; O'Brien, N. M. Protection by the flavonoids myricetin, quercetin, and rutin against hydrogen peroxide-induced DNA damage in Caco-2 and Hep G2 cells. *Nutr. Cancer* **1999**, *34*, 160–166.
(3) Yanez, J.; Vicente, V.; Alcaraz, M.; Castillo, J.; Benavente-Garcia, O.; Canteras, M.; Teruel, J. A. Cytotoxicity and antiproliferative activities of several phenolic compounds against three melanocytes cell lines: relationship between structure and activity. *Nutr. Cancer* **2004**, *49*, 191–199.
(4) Blonska, M.; Czuba, Z. P.; Krol, W. Effect of flavone derivatives on interleukin-1beta (IL-1beta) mRNA expression and IL-1beta protein synthesis in stimulated RAW 264.7 macrophages. *Scand. J. Immunol.* **2003**, *57*, 162–166.
(5) Lu, J.; Papp, L. V.; Fang, J.; Rodriguez-Nieto, S.; Zhivotovsky, B.; Holmgren, A. Inhibition of mammalian thioredoxin reductase by some flavonoids: implications for myricetin and quercetin anticancer activity. *Cancer Res.* **2006**, *66*, 4410–4418.
(6) Zhang, Q.; Zhao, X. H.; Wang, Z. J. Flavones and flavonols exert cytotoxic effects on a human oesophageal adenocarcinoma cell line (OE33) by causing G2/M arrest and inducing apoptosis. *Food Chem. Toxicol.* **2008**, *46*, 2042–2053.
(7) Nadova, S.; Miadokova, E.; Cipak, L. Flavonoids potentiate the efficacy of cytarabine through modulation of drug-induced apoptosis. *Neoplasma* **2007**, *54*, 202–206.
(8) De Leo, M.; Braca, A.; Sanogo, R.; Cardile, V.; De Tommasi, N.; Russo, A. Antiproliferative activity of *Pteleopsis suberosa* leaf extract and its flavonoid components in human prostate carcinoma cells. *Planta Med.* **2006**, *72*, 604–610.
(9) Lee, K. M.; Kang, N. J.; Han, J. H.; Lee, K. W.; Lee, H. J. Myricetin down-regulates phorbol ester-induced cyclooxygenase-2 expression in mouse epidermal cells by blocking activation of nuclear factor kappa B. *J. Agric. Food Chem.* **2007**, *55*, 9678–9684.
(10) Ko, C. H.; Shen, S. C.; Lee, T. J.; Chen, Y. C. Myricetin inhibits matrix metalloproteinase 2 protein expression and enzyme activity in colorectal carcinoma cells. *Mol. Cancer Ther.* **2005**, *4*, 281–290.
(11) Greenlee, R. T.; Hill-Harmon, M. B.; Murray, T.; Thun, M. Cancer statistics. *CA Cancer J. Clin.* **2001**, *51*, 15–36.
(12) Shivapurkar, N.; Reddy, J.; Chaudhary, P. M.; Gazdar, A. F. Apoptosis and lung cancer: a review. *J. Cell Biochem.* **2003**, *88*, 885–898.
(13) Erridge, S. C.; Moller, H.; Price, A.; Brewster, D. International comparisons of survival from lung cancer: pitfalls and warnings. *Nat. Clin. Pract. Oncol.* **2007**, *4*, 570–577.

(14) Murrer, D.; Breathnach, R.; Engelman, A.; Millon, R.; Bronner, G.; Flesch, H.; Dumont, P.; Eber, M.; Abecasis, J. Expression of collagenase related metalloproteinases genes in human lung or head and neck tumors. *Int. J. Cancer* **1991**, *48*, 550–556.
(15) Gontero, P.; Banisadr, S.; Frea, B.; Brausi, M. Metastasis markers in bladder cancer: a review of the literature and clinical considerations. *Eur. Urol.* **2004**, *46*, 296–311.
(16) Parks, W. C.; Shapiro, S. D. Matrix metalloproteinases in lung biology. *Respir. Res.* **2001**, *2*, 10–19.
(17) Foda, H. D.; Zucker, S. Matrix metalloproteinases in cancer invasion, metastasis and angiogenesis. *Drug Discov. Today* **2001**, *6*, 478–482.
(18) Khasigov, P. Z.; Podobed, O. V.; Gracheva, T. S.; Salbiev, K. D.; Grachev, S. V.; Berezov, T. T. Role of matrix metalloproteinases and their inhibitors in tumor invasion and metastasis. *Biochemistry (Moscow)* **2003**, *68*, 711–717.
(19) Duffy, M. J.; Duggan, C. The urokinase plasminogen activator system: a rich source of tumour markers for the individualized management of patients with cancer. *Clin. Biochem.* **2004**, *37*, 541–548.
(20) Itoh, Y.; Nagase, H. Matrix metalloproteinases in cancer. *Essays Biochem.* **2002**, *38*, 21–36.
(21) Westermarck, J.; Kahari, V. M. Regulation of matrix metalloproteinase expression in tumor invasion. *FASEB J.* **1999**, *13*, 781–792.
(22) Aguirre Ghiso, J. A.; Alonso, D. F.; Farias, E. F.; Gomez, D. E.; de Kier Joffe, E. B. Deregulation of the signaling pathways controlling urokinase production. Its relationship with the invasive phenotype. *Eur. J. Biochem.* **1999**, *263*, 295–304.
(23) Chen, P. N.; Hsieh, Y. S.; Chiou, H. L.; Chu, S. C. Silibinin inhibits cell invasion through inactivation of both PI3K-Akt and MAPK signaling pathways. *Chem.−Biol. Interact.* **2005**, *156*, 141–150.
(24) Robinson, M. J.; Cobb, M. H. Mitogen-activated protein kinase pathways. *Curr. Opin. Cell Biol.* **1997**, *9*, 180–186.
(25) Turner, N. A.; Aley, P. K.; Hall, K. T.; Warburton, P.; Galloway, S.; Midgley, L.; O'regan, D. J.; Wood, I. C.; Ball, S. G.; Porter, K. E. Simvastatin inhibits TNFalpha-induced invasion of human cardiac myofibroblasts via both MMP-9-dependent and -independent mechanisms. *J. Mol. Cell Cardiol.* **2007**, *43*, 168–176.
(26) Peng, P. L.; Hsieh, Y. S.; Wang, C. J.; Hsu, J. L.; Chou, F. P. Inhibitory effect of berberine on the invasion of human lung cancer cells via decreased productions of urokinase-plasminogen activator and matrix metalloproteinase-2. *Toxicol. Appl. Pharmacol.* **2006**, *214*, 8–15.
(27) Liotta, L. A.; Steeg, P. S.; Stetler-Stevenson, W. G. Cancer metastasis and angiogenesis: an imbalance of positive and negative regulation. *Cell* **1991**, *64*, 327–336.
(28) Shao, Z. M.; Wu, J.; Shen, Z. Z.; Barsky, S. H. Genistein inhibits both constitutive and EGF- stimulated invasion in ER-negative human breast carcinoma cell lines. *Anticancer Res.* **1998**, *18*, 1435–1439.
(29) Cha, H. J.; Bae, S. K.; Lee, H. Y.; Lee, O. H.; Sato, H.; Seiki, M.; Park, B. C.; Kim, K. W. Anti-invasive activity of ursolic acid correlates with the reduced expression of matrix metalloproteinase-9 (MMP-9) in HT1080 human fibrosarcoma cells. *Cancer Res.* **1996**, *56*, 2281–2284.
(30) Rothhammer, T.; Hahne, J. C.; Florin, A.; Poser, I.; Soncin, F.; Wernert, N.; Bosserhoff, A. K. The Ets-1 transcription factor is involved in the development and invasion of malignant melanoma. *Cell. Mol. Life Sci.* **2004**, *61*, 118–128.

Received for Review January 12, 2009. Accepted March 06, 2009. Revised manuscript received March 5, 2009. This work was supported by the grant from the Center for Regional Industry Academia Collaboration M.O.E., Ministry of Education (96-B-17-042, 97-B-17-018).